

Re-Entry Attitude Two-Loop SMC of the Spacecraft and its Logic Selection

Jie Jia , Fengqi Zhou , Jun Zhou

Abstract—This paper develops a re-entry attitude control method of a Spacecraft by sliding mode control (SMC) theory. The controller utilizes two-loop SMC scheme and provides robust, de-coupled tracking of both the angular velocity and orientation angles of the Spacecraft. And pointing to the blending controlling characteristic of the aerodynamic surfaces and reaction control system of the Spacecraft, allocating the control torque commands into the actuators such as the aerodynamic surfaces and reaction control system by the optimal control logic selection allocation algorithm. Simulation of the Spacecraft re-entry attitude controlling demonstrates robust, de-coupled tracking performance of this method and its validity.

I. INTRODUCTION

RE-ENTRY control of Spacecraft comprises the re-entry attitude manoeuvre through a wide range of flight conditions. The existence of high coupling, wind and poorly understood hypersonic aerodynamics complicate the controller design. Moreover, Sliding mode control(SMC) is a nonlinear control technique that has been actively developed during the past 30-40 years. SMC provides a robust multivariable tracking controlling method of the desired Re-entry attitude control of hypersonic Spacecraft[1-2].

This paper develops a sliding mode controller for a hypersonic Spacecraft, the resulting controller utilizes two-loop sliding mode controller. The frame of this controller is shown in Fig.1. The design process of this controller involves two steps: Firstly, the outer-loop takes the desired angular velocity as dummy input, asymptotically tracking required angular profile. Secondly, the inner-loop uses the control torque as input, tracking required angular velocity profile[3].

Pointing to the characteristic of blending control of the aerodynamic surface and reaction control system(RCS) of Re-entry attitude control of hypersonic Spacecraft, an optimal control allocation algorithm is employed to allocate control torques into end-effectors, which are executed by the actuators separately. Simulation of the Spacecraft demonstrated accurate, robust, decoupled tracking performance and its validity.

Jie Jia is presently a doctoral candidate in College of Astronautics, Northwestern Polytechnical University, Xi'an, China(phone: 086-029-88486080, fax: 086-029-88486080; e-mail: jiejie757@npu.edu.cn).

Fengqi Zhou is with the College of Astronautics, Northwestern Polytechnical University, Xi'an China.

Jun Zhou is with the College of Astronautics, Northwestern Polytechnical University, Xi'an China.

II. THE EQUATIONS OF SPACECRAFT MOTION

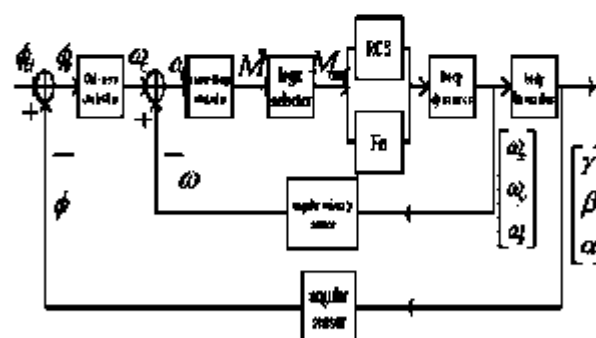


Fig. 1. Controller Frame

The equations of Spacecraft motion in re-entry mode are given by the Euler equation[2]:

$$\underline{I} \frac{d\omega}{dt} + \omega \times (\underline{I} \cdot \omega) = \underline{M}_c + \underline{M}_d \quad (1)$$

$$\dot{\phi} = R(\cdot) \omega \quad (2)$$

$$\dot{y} = \phi \quad (3)$$

Where, $\underline{I} \in R^{3 \times 3}$ is the symmetric, positive definite moment of inertia tensor, $\omega = [\omega_x \ \omega_y \ \omega_z]^T$ is the angular rate vector, $\underline{M}_c \in R^{3 \times 1}$ is the control torque vector.

$\underline{M}_d \in R^{3 \times 1}$ contains any external disturbance torque vector.

$\phi = [\gamma \ \beta \ \alpha]^T$, γ, β, α are the bank, sideslip and angle of attack respectively. The matrix $R(\cdot)$ in the re-entry

mode is given by: $R(\cdot) = \begin{bmatrix} 0 & 0 & 1 \\ \sin \alpha & \cos \alpha & 0 \\ \cos \alpha & -\sin \alpha & 0 \end{bmatrix}$, y is the output vector.

III. TWO-LOOP SMC DESIGN

The problem is to determine the control input \underline{M}_c , so that the desired Spacecraft angle $\phi_d(t)$ are robustly followed regardless bounded disturbance and modeling uncertainties

[3].

A. Outer-Loop SMC Design

In order to design a suitable outer-loop SMC controller, taking the angular velocity vector ω in (2) as dummy control input ω_c to asymptotic track desired attitude angular ϕ_d , accordingly determine ω_c . And then ω_c is followed by the inner-loop controller.

Selecting the switching surface of the SMC:

$$s_w = e_w + K_w \int_0^t e_w d\tau = 0 \quad (4)$$

$$\text{where, } e_w = \phi_d - \phi = y_d - y$$

$$K_w = \text{diag}\{k_i\}, K_w \in R^{3 \times 3}$$

In order to ensure the system trajectory asymptotic convergence to the switching surface of the SMC, the dummy control input ω_c must be designed. The derivative of (4) is:

$$\dot{s}_w = \dot{e}_w + K_w e_w = \dot{\phi}_d - \dot{\phi} + K_w e_w \quad (5)$$

Substituting (2) into (5) and selecting the trending law $\dot{s}_w = \rho \cdot \text{SIGN}(s_w)$, educing:

$$\omega_c = R^{-1}(\cdot) [\dot{\phi}_d + K_w e_w] + R^{-1}(\cdot) \rho \cdot \text{SIGN}(s_w) \quad (6)$$

where

$$\text{SIGN}(s_w) = [\text{sign}(s_{w1}) \quad \text{sign}(s_{w2}) \quad \text{sign}(s_{w3})]^T, \rho > 0$$

Obviously, the angular velocity command (6) is discontinuous and will chatter while on the sliding surface. Certainly, such angular velocity can not be tracked by the inner-loop controller of the Spacecraft.

To avoid the sliding mode chatter phenomena, a outer-loop approximative continuous SMC with a boundary layer is utilized. At the same time, to ensure finite-reaching-time convergence of the system's trajectory to ε -vicinity of the sliding surface, $\text{SIGN}(s_w)$ is substituted by the continuous term[4].

$$f\left(\frac{s_{wi}}{\varepsilon_{wi}}\right) \cdot \text{SAT}\left(\frac{s_{wi}}{\varepsilon_{wi}}\right) = \left\{ f_1\left(\frac{s_{w1}}{\varepsilon_{w1}}\right) \text{sat}\left(\frac{s_{w1}}{\varepsilon_{w1}}\right) \quad f_2\left(\frac{s_{w2}}{\varepsilon_{w2}}\right) \text{sat}\left(\frac{s_{w2}}{\varepsilon_{w2}}\right) \quad f_3\left(\frac{s_{w3}}{\varepsilon_{w3}}\right) \text{sat}\left(\frac{s_{w3}}{\varepsilon_{w3}}\right) \right\}^T$$

where

$$\text{sat} \frac{s_{wi}}{\varepsilon_{wi}} = \begin{cases} 1 & s_{wi} > \varepsilon_i \\ \frac{s_{wi}}{\varepsilon_{wi}} & |s_{wi}| \leq \varepsilon_i \\ -1 & s_{wi} < -\varepsilon_i \end{cases}$$

$$f_i\left(\frac{s_{wi}}{\varepsilon_{wi}}\right) = -2 \frac{\varepsilon_{wi} + 1}{2} \left| \frac{s_{wi}}{\varepsilon_{wi}} \right|^{\varepsilon_{wi}}$$

Obtaining the outer-loop continuous SMC as follows:

$$\omega_c = R^{-1}(\cdot) [\dot{\phi}_d + K_w e_w] + R^{-1}(\cdot) \rho \cdot f\left(\frac{s_w}{\varepsilon_w}\right) \cdot \text{SAT}\left(\frac{s_w}{\varepsilon_w}\right) \quad (7)$$

B. Inner-Loop SMC Design

After determining ω_c , designing the inner-loop SMC controller to track ω_c :

$\lim_{t \rightarrow \infty} \|\omega_c - \omega\| = 0, \forall i = 1, 2, 3$, so as to obtain the desired profile of the inner-loop SMC.

Selecting the switching surface of the inner-loop SMC:

$$s_n = \omega_c - \omega + K_n \int_0^t \omega_c d\tau = 0 \quad (8)$$

where

$$\omega_c = \omega_c - \omega, K_n = \text{diag}\{k_n\}, K_n \in R^{3 \times 3}$$

Design the control input M_c to make the trajectory of equation (1) asymptotic converge to the switching surface of the SMC. Substituting (1) into the derivative equation of (8):

$$\dot{s}_n = \dot{\omega}_c + I^{-1}(\omega \times I \omega) - I^{-1} M_c - I^{-1} M_d + K_n \omega_c = 0$$

Selecting the trending law $\dot{s}_n = \rho \cdot \text{SIGN}(s_n)$, educing:

$$M_c = I \dot{\omega}_c + \omega \times I \omega - M_d + [K_n \omega_c - I \rho \cdot \text{SIGN}(s_n)] \quad (9)$$

To avoid the control torque chatter phenomena, utilizing a inner-loop approximative continuous SMC with a boundary layer. At the same time, to ensure finite-reaching-time convergence of the system's trajectory to ε -vicinity of the sliding surface, $\text{SIGN}(s_n)$ is substituted by the continuous term[4].

$$f\left(\frac{s_{ni}}{\varepsilon_{ni}}\right) \cdot \text{SAT}\left(\frac{s_{ni}}{\varepsilon_{ni}}\right) = \left\{ f_1\left(\frac{s_{n1}}{\varepsilon_{n1}}\right) \text{sat}\left(\frac{s_{n1}}{\varepsilon_{n1}}\right) \quad f_2\left(\frac{s_{n2}}{\varepsilon_{n2}}\right) \text{sat}\left(\frac{s_{n2}}{\varepsilon_{n2}}\right) \quad f_3\left(\frac{s_{n3}}{\varepsilon_{n3}}\right) \text{sat}\left(\frac{s_{n3}}{\varepsilon_{n3}}\right) \right\}^T$$

$$\text{sat} \frac{s_{ni}}{\varepsilon_{ni}} = \begin{cases} 1 & s_{ni} > \varepsilon_{ni} \\ \frac{s_{ni}}{\varepsilon_{ni}} & |s_{ni}| \leq \varepsilon_{ni} \\ -1 & s_{ni} < -\varepsilon_{ni} \end{cases}$$

where

$$f_i\left(\frac{s_{ni}}{\varepsilon_{ni}}\right) = -2 \frac{\varepsilon_{ni} + 1}{2} \left| \frac{s_{ni}}{\varepsilon_{ni}} \right|^{\varepsilon_{ni}}$$

Obtaining the inner-loop continuous SMC as follows:

$$M_c = I \dot{\omega}_c + \omega \times I \omega - M_d + [K_n \omega_c - I \rho \cdot f\left(\frac{s_n}{\varepsilon_n}\right) \cdot \text{SAT}\left(\frac{s_n}{\varepsilon_n}\right)] \quad (10)$$

IV. BLENDING CONTROL ALLOCATOR

As the Spacecraft begins its descent, due to the fins efficiency are low, the attitude control rely on RCS entirely. To minimize fuel consumption, the mission of attitude control is done by the fins to the best of it's abilities. This requires a logic selection allocator to estimate how much control authority the fins are capable of at any time, and to carry through blending control allocation until the fins can take on the control action.

Blending control allocator is shown in Fig.2, where \underline{T} is the control conversion matrix. Selector calculates the aerodynamics press q to estimate when the fins participate in the attitude control. The actuator command \underline{M}_{cmd} is passed through a position limiter to produce the final aerodynamic surface command $\underline{\delta}_{aero}$. Multiplying $\underline{\delta}_{aero}$ by \underline{T} is $\underline{a}_{available}^*$ estimate whether $\underline{a}_{available}^*$ is equal to the $\underline{a}^* = \underline{M}^* \underline{T}$. If \underline{M}_{cmd} is larger than the position limit, then the difference between $\underline{a}_{available}^*$ and \underline{a}^* can be taken as

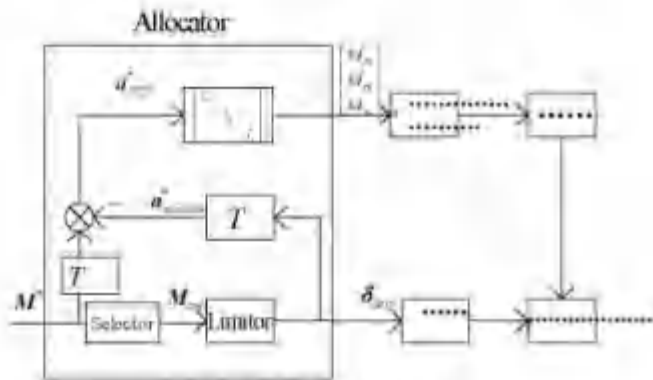


Fig. 2. Blending Control Allocator

acceleration command, this command is converted to RCS by the inertia matrix, the allocation process is shown in Fig 2. Due to the limit of length, the Reaction control logic is not discussed in this paper.

V. SIMULATION OF RE-ENTRY ATTITUDE

The inertia matrix of spacecraft re-entry is as follows:

$$\underline{I} = \begin{bmatrix} 554,486 & 0 & -23,002 \\ 0 & 1,136,949 & 0 \\ -23,002 & 0 & 1,376,852 \end{bmatrix} \text{ kg} \cdot \text{m}^2$$

To validate the robust of this controller, a dummy high amplitude, frequency external disturbances are utilized:

$$\mathbf{M}_d = [10^5 \sin(t) \quad 10^5 \sin(t) \quad 10^5 \sin(t)], Nm$$

The desired angular command is the signum function. The desired attitude command, practice attitude response, dummy

angular velocity input and practice angular velocity response, required control torque of the simulation are shown in Fig.3-10. It can be shown that the attitude angular can track the caustic signum function very well.

VI. CONCLUSIONS

In this paper, the re-entry attitude control of Spacecraft and logic selection problem are discussed. To avoid command chatter phenomenon, at the same time, to ensure finite-reaching-time convergence of the system's trajectory to ε -vicinity of the sliding surface, utilizing a two-loop SMC framework to design continuous finite-time SMC, the output of the SMC are control torque.

And pointing to the blending control of the aerodynamic surface and reaction control system(RCS) of Re-entry attitude control of hypersonic Spacecraft, an optimal control allocation algorithm is employed. In order to validate the robust and validity of this controller, a dummy high amplitude, frequency external disturbances are introduced. Simulation of the Spacecraft demonstrated accurate, robust, decoupled tracking performance of this method and its validity.

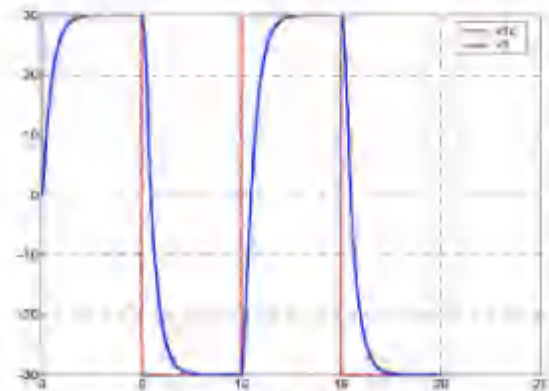
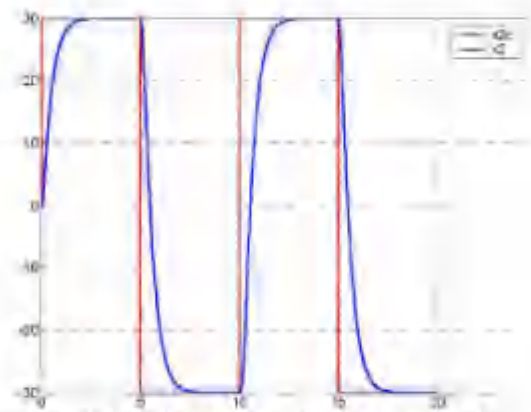


Fig. 3 Bank angular tracking response(deg)



*****Fig.4 Slidstep angular tracking response(deg)*****

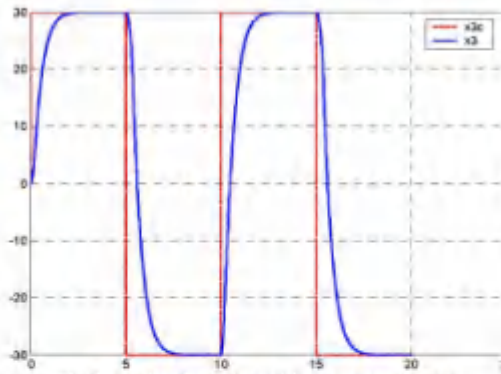


Fig.5. Angle of attack tracking response(deg)••

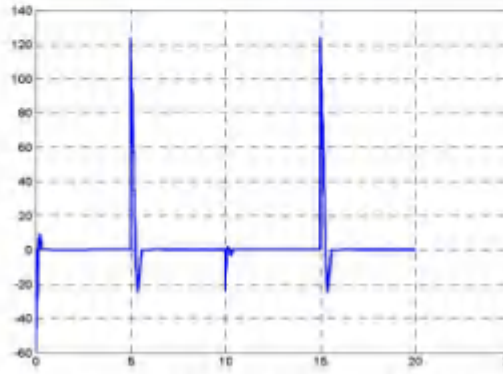


Fig.6. Error of ω_{wx} and ω_x (deg/s)••

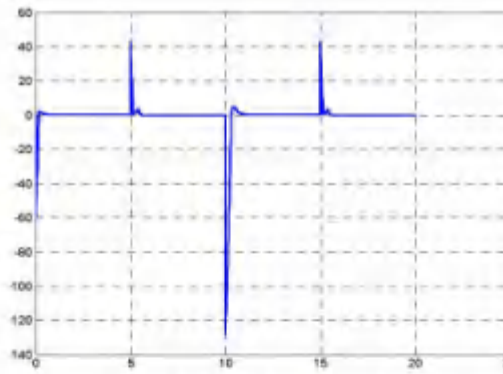


Fig.7. Error of ω_{cy} and ω_y (deg/s)••

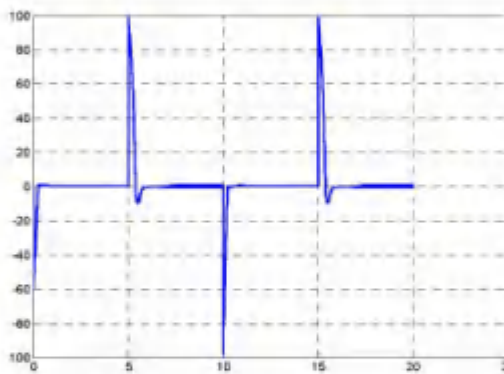


Fig.8. Error of ω_{cz} and ω_z (deg/s)••

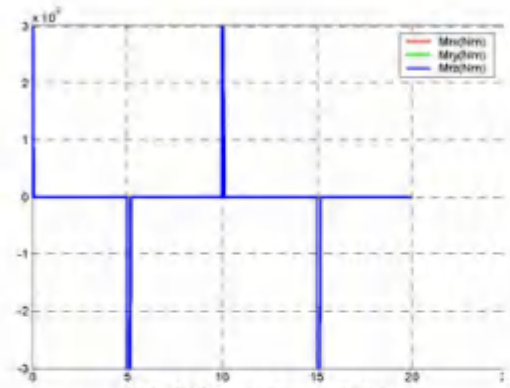


Fig.9. RCS control torque(Nm)••

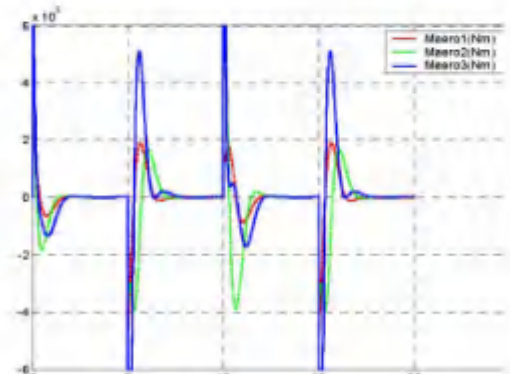


Fig.10. Aerodynamics surface torque(Nm)••

REFERENCES

- [1] J. Zhou, F. Q. Zhou, "A New Autopilot Design Method for Bank to Turn Missiles Based on the Variable Structure Control Theory," Bei-Jing: Journal of astronautics, vol. 1, Feb. 1994, pp.42-47.
- [2] H. Y. Zhao, *The Dynamics and Guidance of Re-Entry Aircraft*. Changsha: National University of Defence Technology Press, 1997, 84-86.
- [3] U. Itkin, *Control system of Variable Structure*. New York: Wiley, 1976.
- [4] Y. Shtessel and J. Buffington, "Continuous Sliding Mode Control," Proceedings of the American Control Conference, 1998, pp. 562-563.